PERGAMON

Acta mater. Vol. 47, No. 9, pp. 2661–2668, 1999

Printed in Great Britain
PII: S1359-6454(99)00137-8
1359-6454/99 $20.00 + 0.00

ON BOUNDARY MISORIENTATION DISTRIBUTION FUNCTIONS AND HOW TO INCORPORATE THEM INTO THREE-DIMENSIONAL MODELS OF MICROSTRUCTURAL EVOLUTION

M. MIODOWNIK[1]†, A. W. GODFREY[2], E. A. HOLM[1] and D. A. HUGHES[2]

[1]Sandia National Laboratories, Albuquerque, NM 87185, U.S.A. and [2]Sandia National Laboratories, Livermore, California, U.S.A.

(Received 21 January 1999; accepted 27 April 1999)

Abstract—The fundamental difficulties of incorporating experimentally obtained boundary misorientation distributions (BMDs) into three-dimensional microstructural models are discussed. An algorithm is described which overcomes these difficulties. The boundary misorientations are treated as a statistical ensemble which is evolved toward the desired BMD using a Monte Carlo method. The application of this algorithm to a number of complex arbitrary BMDs shows that the approach is effective for both conserved and non-conserved textures. The algorithm is successfully used to create the BMDs observed in deformation microstructures containing both incidental dislocation boundaries (IDBs) and geometrically necessary boundaries (GNBs). The application of an algorithm to grain boundary engineering is discussed.

Keywords: Grain boundaries; Microstructure; Computer simulation

1. INTRODUCTION

At a recent international meeting on grain growth and related phenomena [1] a panel discussion was convened to debate issues of current importance to the field. One topic raised concerned the need to incorporate real microstructures as starting configurations for computer models of various kinds. A primary aspect of this is the inclusion of the full crystallographic diversity of the grain or sub-grain structures to be modeled. At the simplest level this can be achieved by discretizing an experimentally obtained orientation distribution function (ODF) and then assigning orientations to individual elements within a computer model using a weighting scheme based on the discretized ODF. In addition to the crystallographic texture, increasing importance is being given to the grain boundary texture, that is to say the distribution of grain boundary characteristics within a given material. The increased focus on grain boundary texture reflects the recognition that many material properties can be significantly enhanced by careful control of the grain boundary characteristics [2, 3]. Incorporation of representative grain boundary texture is also necessary for improving models of processes where the underlying physical properties are known to vary as a function of grain boundary character [4, 5]. As our knowledge base of grain boundary property–structure relationships is expanded, the requirement to include experimental grain boundary textures in computer models will only increase.

The full grain boundary texture covers a large parameter space, consisting both of the relative misorientation of two crystallites, the inclination of the boundary plane (which for curved boundaries will vary at each point), and potentially the translational displacements between the two crystallites. Whilst it is known that properties may vary with each of these parameters, attention has been predominantly focused on the relative misorientation of the crystallites [6–8]. The grain boundary texture described in this way has been termed the grain boundary misorientation distribution. The relative misorientation between crystallites is most commonly expressed by an angle of rotation about an axis common to both crystallites that brings one into coincidence with the other (the angle:axis pair description) though other descriptions (notably that using the Rodriguez–Frank vector) are possible and may in cases be more appropriate [9, 10].

The most direct method for incorporating both experimental textures and grain boundary textures into computer models is to utilize a discretized lattice model and to then make a one-to-one correlation with spatially resolved orientation data gathered experimentally. Such data can be provided by backscattered Kikuchi pattern methods in the scanning electron microscope, which have been developed to the point where large areas can be

†To whom all correspondence should be addressed.

investigated in relatively short times with a spatial resolution of less than a micron [11–13]. The philosophy of this approach is to provide an "image" of an experimental microstructure that can be fed exactly into a computer model, thus allowing immediate comparison of the microstructure evolution predicted by the model with the experimental material evolution. This technique is practically limited to two-dimensional measurements; extension to three dimensions requires serial sectioning techniques combined with reconstruction algorithms to account for the material removed between each section. In many cases, however, it is sufficient to use a statistical description of the microstructure where both the texture and boundary misorientation distribution are described by suitably defined probability density functions. Such data can be gathered from either line scans or area scans in the scanning electron or transmission electron microscope [14–17].

In this paper we describe a method for constructing discrete, topologically correct, initial microstructures based on such a statistical description of the boundary misorientation distributions. The descriptions above and the methodology to be applied are equally valid for any system of single phase boundaries (e.g. between grains, dislocation cells, recovered subgrains). To emphasize this point we refer in the text only to the boundary misorientation distribution (BMD) and use the term *domain* to represent either grains, cells or subgrains.

One inherent problem with assigning a system of misorientations is that it is not possible to allocate misorientations to every boundary independently — the net rotation at a triple junction must be zero at equilibrium, and hence there exists a correlation between misorientations in any topologically linked set of grains. This problem, and its solution, is discussed further in the next section. Later we describe how BMDs can be classified and illustrate how the algorithm developed can be applied to create each type of BMD.

2. THE METHOD

2.1. Boundary misorientation distributions

We take a three-dimensional polycrystal microstructure generated from a Potts model simulation of grain growth [18, 19], see Fig. 1. This has the topology and domain size distribution of an equiaxed grain structure with 3084 (N_g) domains and 22 311 (N_b) boundaries. Each of the N_g domains is assigned a crystallographic cubic orientation expressed as a 3×3 matrix of direction cosines $\mathbf{O}_i$ [20]. A list of pairs of domains is generated which define the N_b boundaries present in the system and a misorientation matrix $\mathbf{M}_{ij}$ between each pair is calculated such that

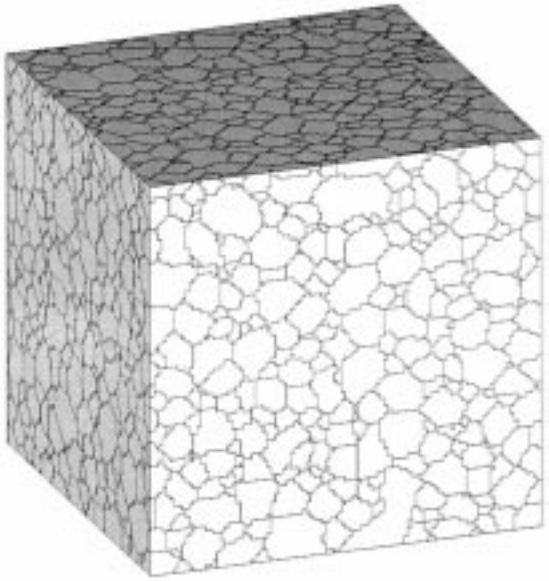

Fig. 1. A three-dimensional equiaxed microstructure obtained from a computer simulation of grain growth. The structure is used to compute the list of grain boundaries present in the system.

$$\mathbf{M}_{ij} = \mathbf{O}_i \mathbf{O}_j^{-1} \tag{1}$$

where $\mathbf{O}_i$ and $\mathbf{O}_j$ are the orientations of domains i and j. This misorientation is then expressed in angle:axis format, taking the solution with the minimum misorientation angle from the equivalent descriptions allowed by cubic symmetry. This defines the disorientation angle:axis pair between domains i and j as θ_{ij}:$[uvw]_{ij}$. The disorientation angle:axis pair is calculated for every boundary and the BMD function describing the probability of finding a boundary in the system with given disorientation angle, is defined such that $P(\theta, \Delta\theta)$ is the fraction of boundaries with disorientation angles between θ and $\theta + \Delta\theta$.

Textures are incorporated by discretizing orientation space so that a given texture is expressed by N_g orientations. The method by which one initially allocates these orientations to the N_g domains in the ensemble determines the BMD. By allocating random orientations to the domains, a $\mathrm{BMD}_{\mathrm{rand}}$ is produced. This is just the Mackenzie distribution [21]. One can however distribute these same orientations in a non-random manner, for instance by choosing to give neighboring domains orientations which are close in Euler space. In doing so one produces a BMD with a high proportion of low angle boundaries. Just as easily, one could choose to bias the BMD towards high angle boundaries. Thus, the BMD is not unambiguously defined by the texture, it also depends on the correlation between adjacent orientations. To illustrate this we constructed an algorithm, similar to one described by Kiewel *et al.* [22], which picks two domains at random from the microstructure and

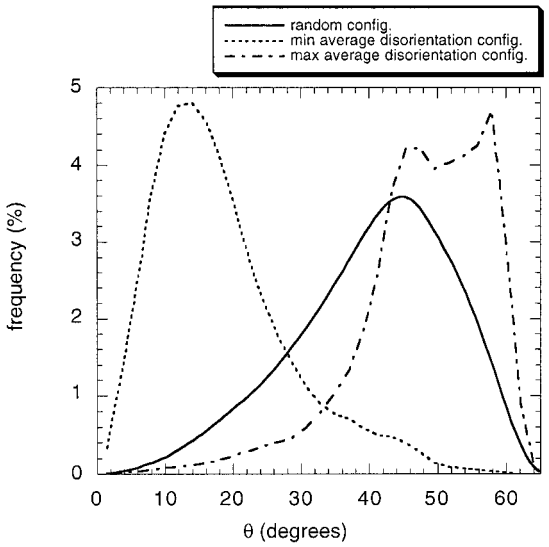

Fig. 2. BMDs of randomly textured polycrystals with different types of neighbor correlation.

swaps their orientations if the average disorientation of the microstructure is decreased. We stopped when no further swaps could be found that decreased the average disorientation. Similarly we used the same approach to find the configuration that maximized the average disorientation (accepting swaps that increased the average disorientation of the system). The final boundary misorientation distributions of the minimum and maximum average disorientation configurations, BMD_{min} and BMD_{max}, respectively, are shown in Fig. 2, thus illustrating the wide range of BMDs that can be obtained from a random texture. The average misorientations of BMD_{rand}, BMD_{min}, and BMD_{max} are 40.7°, 18.2°, and 47.9°, respectively.

2.2. Tailoring a BMD using a Monte Carlo algorithm

Constructing a specific BMD given the texture and microstructure is a non-trivial task. It is necessary to allocate orientations to the domains in such a way that the frequency of boundaries with a particular disorientation conform to that given by the BMD. However, the misorientation of each grain boundary cannot be uniquely defined. Figure 3 shows a two-dimensional section through the three-dimensional equiaxed microstructure of Fig. 1. We are free to pick any orientation for domain 1, and then we can pick an orientation for domain 2 to determine θ_{12}. If we then pick an orientation for domain 3, θ_{13} and θ_{23} are determined simultaneously. Thus θ_{13} and θ_{23} are correlated. There is no way of ensuring, in any general scheme of orientation allocation, that we can always pick the orientation of domain 3 so that θ_{13} and θ_{23} are both misorientations we require in the desired BMD.

We propose the following methodology to overcome this problem. BMDs are quantized into n bins, such that S_k is the number of boundaries with disorientations between $k\Delta\theta$ and $(k+1)\Delta\theta$, $k = 0, 1, \ldots, n$. We allocate arbitrarily N_g orientations which describe the texture to each of the N_g domains. A system Hamiltonian is defined as the sum of the squared differences between S_k^m and S_k^d:

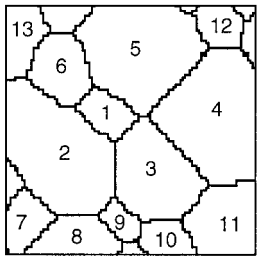

Fig. 3. Part of a two-dimensional section of Fig. 1 showing the topology of the grain structure of an equiaxed system.

$$H_S = \sum_{k=0}^{k=n} (S_k^m - S_k^d)^2 \tag{2}$$

where S_k^m defines the BMD of the model and S_k^d defines the desired BMD we are trying to reproduce. H_S is a state variable providing a measure of the difference between the model BMD and the desired BMD. It is equal to zero when the model BMD and the desired BMD are identical.

We use a Monte Carlo algorithm in order to minimize H_S and in doing so construct the desired BMD. The method is as follows: two domains are chosen at random, and the ΔH_S due to swapping their orientations is calculated. The probability $p(\Delta H_S)$ that the swap is accepted is governed by the probability function

$$p(\Delta H_S) = \begin{cases} 1 & (\Delta H_S \leq 0) \\ \exp[-\Delta H_S/\beta] & (\Delta H_S > 0) \end{cases} \tag{3}$$

where β is a constant analogous to a thermal energy in thermodynamic systems [23]. In the current work $\beta = 0$ was used and hence only swaps that reduced H_S were accepted. N_b attempted swaps are defined as a single Monte Carlo time step (MCS). Swaps are attempted until the time derivative of H_S approaches zero.

This algorithm conserves texture but it can be modified to produce a non-conserved texture version in which a domain is chosen and allocated a random orientation. In the same way as the conserved texture model, a ΔH_S is calculated for the change and accepted with a probability determined by equation (3).

3. APPLICATIONS

3.1. Conserved texture

For the purpose of illustrating the use of the technique we defined three BMDs and then used the Monte Carlo algorithm to create a microstruc-

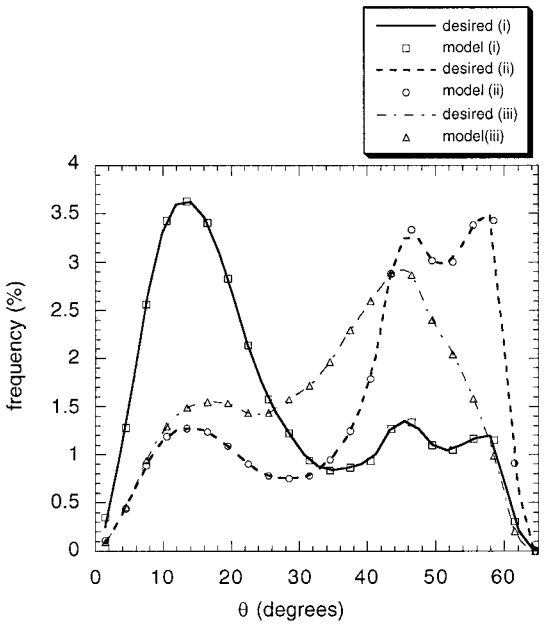

Fig. 4. A comparison of the desired and model BMDs (i), (ii) and (iii), as specified in the text. The model BMD was obtained using the conserved texture algorithm.

ture which exhibited these BMDs. The desired BMDs were created from linear combinations of BMD_{min}, BMD_{max}, and BMD_{rand}, see Fig. 4:

(i) $S_k^d = 0.25BMD_{max} + 0.75BMD_{min}$.
(ii) $S_k^d = 0.75BMD_{max} + 0.25BMD_{min}$.
(iii) $S_k^d = 0.75BMD_{rand} + 0.25BMD_{min}$.

Random orientations were allocated to the domains in the microstructure shown in Fig. 1, using the quarternion method [24]. This defined randomly the disorientations of the boundaries and hence the initial BMD of the model, S_k^m. For each of the three desired BMDs, S_k^d was calculated and the model evolved using the conserved texture Monte Carlo algorithm. Good agreement between the BMDs of the model and the desired BMDs was achieved after 100 MCS, see Fig. 4.

3.2. Non-conserved texture

Using a non-conserved texture algorithm places less contraint on the type of BMD that can be created. Since the number of possible BMDs is almost infinite we present only a couple of examples to illustrate the technique.

Firstly we transform the Mackenzie distribution to one where all misorientations have an equal probability of occurring in the microstructure. Each grain was given an initial random orientation, and the system then allowed to evolve using the unconserved texture algorithm. Figure 5 compares the BMD created by the model and the desired BMD after 1000 MCS at which point further changes in H_S became logarithmically slow. The model BMD matches the desired BMD except at very high and

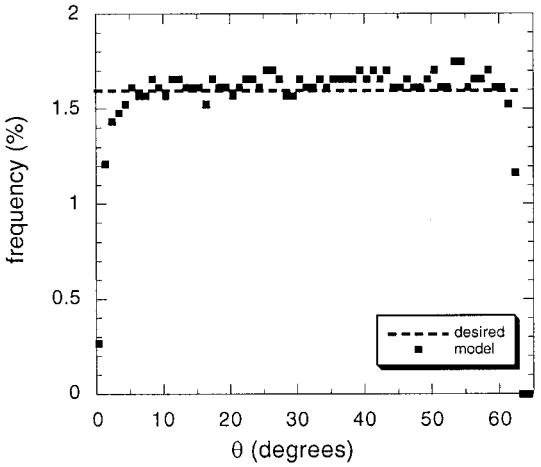

Fig. 5. A comparison of BMDs where all the misorientations have the same probability of occurring in the microstructure. The model BMD was obtained using the unconserved texture algorithm.

very low misorientations. This difference is likely to be a constraint effect arising from the difficulty in matching a sharp probability function. The success of the algorithm is seen also in the second case where we evolved a BMD step function, defined in this case to consist of misorientations only between 1° and 2°. Figure 6 shows the comparison between the desired and model BMDs after 1000 MCS.

3.3. BMDs of dislocation cell block structures

Whilst it is sufficient in most cases to consider that only one type of boundary exists within the microstructure, there are some cases where the structure to be replicated consists of more than one type of boundary, each type having both its own morphological and misorientation distribution characteristics. One case would be a continuous recovery structure in which there exists a distribution of grains with a certain characteristic misorientation distribution, with the subgrains having

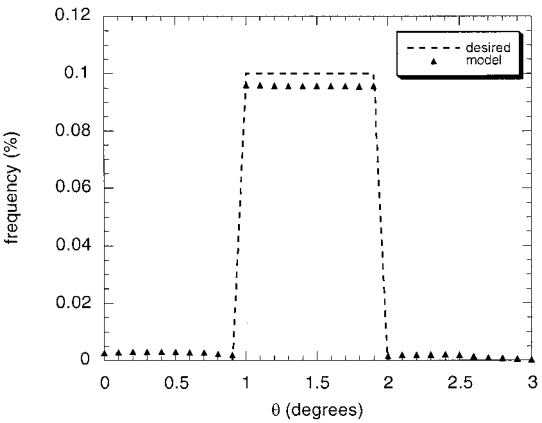

Fig. 6. A comparison of step function BMDs. The model BMD was obtained using the unconserved texture algorithm.

different misorientation distribution characteristics. This subject has been reviewed by Humphreys and Hatherly [25]. Another example, and the one that we present here, is that of dislocation cell block structures in medium to high stacking fault energy f.c.c. materials [16, 17]. Dislocations developed during monotonic plastic deformation of such materials often organize into boundaries that subdivide an original grain at two length scales. The larger scale is defined by long, continuous dislocation boundaries which have been called geometrically necessary boundaries (GNBs). Within the block shaped volumes defined by these boundaries smaller scale cell boundaries, termed incidental dislocation boundaries (IDBs), are formed. The misorientation angle distributions of GNBs and IDBs each evolve differently as a function of strain. There is a further twist in this particular case in that Hughes *et al.* [16, 17] have shown that for a wide range of f.c.c. materials the misorientation angle distributions of the IDBs and the GNBs exhibit a scaling property. Thus the misorientation distribution functions are dependent only on the average misorientation, θ_{av}, and so the varying distributions collapse onto to a single curve when scaled by θ_{av}. This function has been determined empirically as

$$f\left(\frac{\theta}{\theta_{\mathrm{av}}}\right) = \frac{\alpha^{\alpha}}{\Gamma(\alpha)}\left(\frac{\theta}{\theta_{\mathrm{av}}}\right)^{\alpha-1}\exp\left(-\alpha\left(\frac{\theta}{\theta_{\mathrm{av}}}\right)\right) \qquad (4)$$

where $\Gamma(\alpha)$ is the gamma function evaluated at argument α (the fitting parameter), using $\alpha = 3$ for the IDBs and $\alpha = 2.5$ for the GNBs. One implication of this work is that the IDB and GNB distributions at a given strain can be calculated from a knowledge of the evolution of just the average values with strain. Similarly we can use only the average values to reproduce an experimental microstructure.

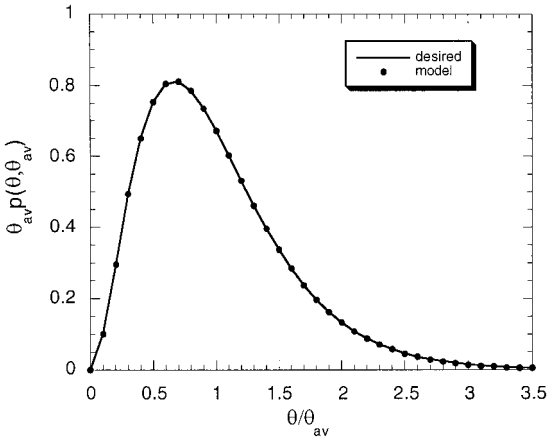

Fig. 7. A comparison of BMDs for the IDBs. The model BMD was obtained using the unconserved texture algorithm.

The IDB distribution shape for a value of $\theta_{\mathrm{av,IDB}} = 1^{\circ}$ was calculated using equation (4) and the fit value of $\alpha = 3.0$. The initial configuration was then evolved towards this target distribution using the non-conserved texture algorithm. Excellent agreement between the desired and the model distribution is achieved after 100 MCS, see Fig. 7.

As noted above the deformation microstructures also contain GNBs, having a different scaling form ($\alpha = 2.5$) and with $\theta_{\mathrm{av,GNB}}$ evolving differently with strain than for the IDBs. Although IDBs and GNBs are distinct features of the microstructure, some dislocation cells will have both these types of boundaries. Therefore, the misorientation angle distributions of the IDBs and GNBs are coupled.

GNBs were incorporated in the polycrystal by inserting a series of parallel planar boundaries into the lattice — an idealization of the observed experimental morphology. The simplest case is illustrated in Fig. 8. Due to the continuous boundary conditions applied, this corresponds to a microstructure with a series of planar boundaries separated by a distance of half the simulation size. We then defined two sets of boundaries in the structure, corresponding to IDBs and GNBs. These were treated as two separate boundary sets each with its own misorientation angle distribution, thus defining $S_k^{\mathrm{m-IDB}}$ and $S_k^{\mathrm{m-GNB}}$. As in the experimental case, some cells had both IDB and GNB faces. For these cells, any orientation change affects both the IDB and GNB misorientation angle distributions. The Hamiltonian was accordingly modified to:

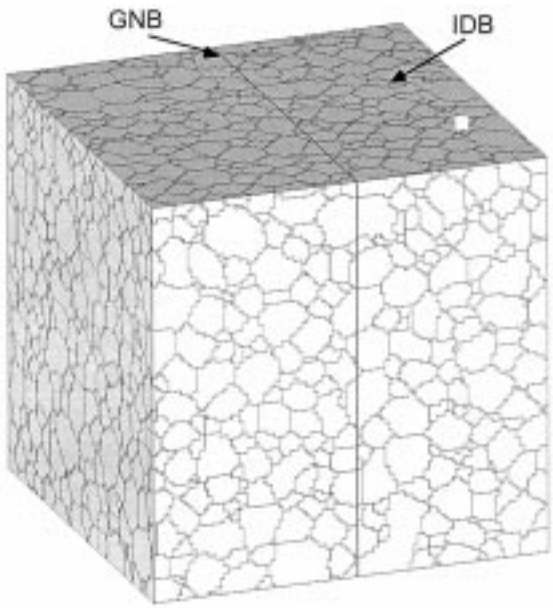

Fig. 8. A three-dimensional polycrystal containing planar GNB features and equiaxed IDB delineated cells.

$$H_S = \sum_{k=0}^{k=n} (S_k^{\mathrm{m-IDB}} - S_k^{\mathrm{d-IDB}})^2 + (S_k^{\mathrm{m-GNB}} - S_k^{\mathrm{d-GNB}})^2. \quad (5)$$

The aim was to optimize the misorientation angle distributions of the IDBs and the GNBs to match the experimental scaling function with $\theta_{\mathrm{av,IDB}} = 1^\circ$ and $\theta_{\mathrm{av,GNB}} = 5^\circ$. The grains of the polycrystal are naturally divided into two sets by the insertion of the GNB boundary. As before we allocated a starting orientation, but this time we gave the cells on the right of the GNB a texture with a 1° spread from a reference orientation $\mathbf{O}_{\mathrm{ref1}}$ and the cells on the other side of the GNB a texture with a 1° spread from $\mathbf{O}_{\mathrm{ref2}}$. The two reference orientations were chosen to give the GNB boundaries an initial average misorientation of approximately 5°. Figure 9 shows the initial misorientation angle distributions of both sets of boundaries. It can be seen that although the IDB distribution is close to the desired function the GNB distribution is way off. The IDB and GNB distributions, after evolving the systems for 1000 MCS using the Hamiltonian of equation (5), are shown in Fig. 10. It can be seen that optimization of both misorientation distributions was largely successful. There is some deviation of the GNB misorientation distribution from the desired function; this is due to the constraints imposed by the IDB distribution.

It should be noted that using experimental data obtained from two-dimensional sections and incorporating them into a three-dimensional model assumes that the two-dimensional sections are stereologically representative. We checked this assumption by taking two-dimensional slices of our model and measuring the BMD of the exposed domains. These matched the three-dimensional data exactly.

4. DISCUSSION

The example of incorporating two types of boundaries illustrates how the complexity of real microstructures can be successfully incorporated into microstructural models using the algorithm presented in this paper. We have also shown that one can use the model to construct microstructures with artificial BMDs. It is envisioned that this might be a useful tool for those using grain boundary engineering to improve materials properties. Corrosion resistance [2] and fracture toughness [26] have been found to be highly dependent on grain boundary character. By allowing the construction of microstructures with specific BMDs the algorithm can be used in conjuction with a materials model to systematically investigate the effect of the BMD function on materials properties.

The most important further development of the model will be extension to include the coincident site lattice (CSL) boundary misorientation

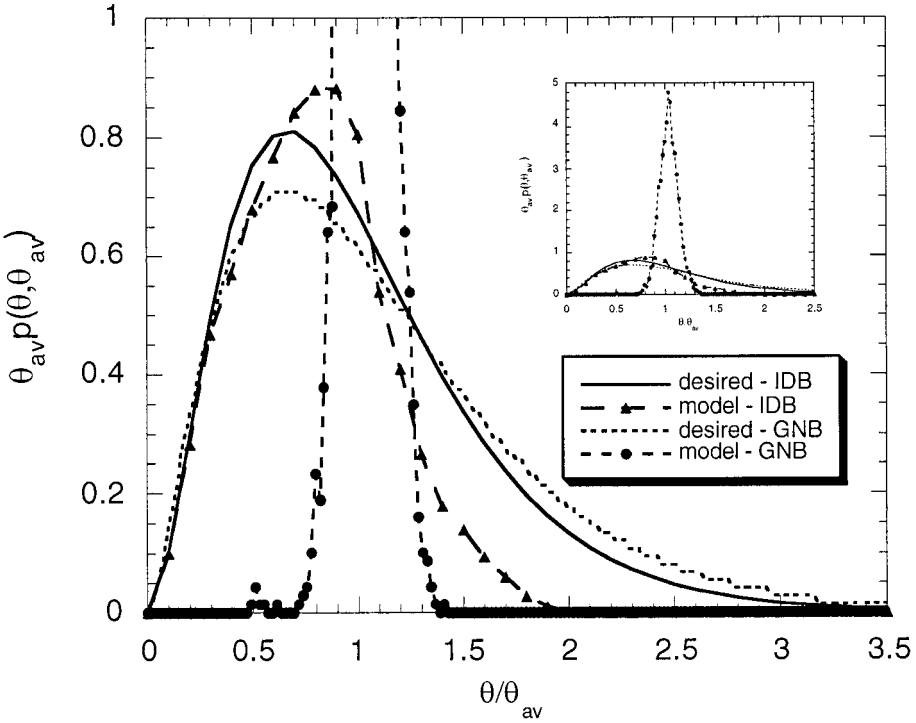

Fig. 9. A comparison of the initial IDB and GNB misorientation distributions before application of the algorithm.

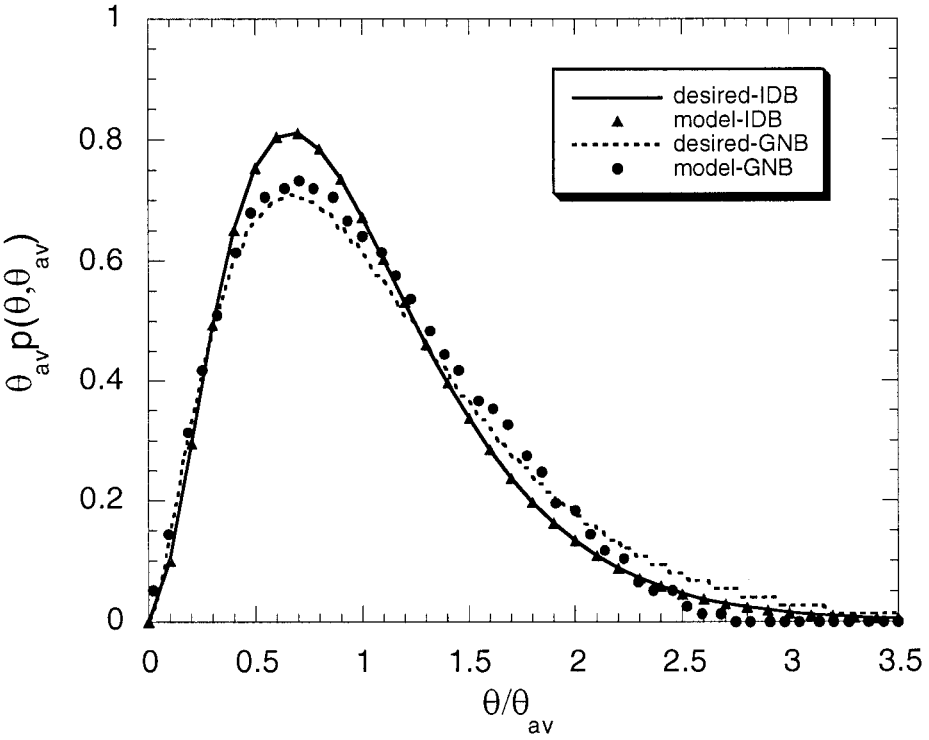

Fig. 10. A comparison of IDB and GNB misorientation distributions after application of the algorithm. The BMDs were obtained using the unconserved texture algorithm.

description [27]. The CSL description of misorientations is a purely geometric model based on the fact that for certain very specific misorientations of one lattice to another, a fraction of the lattice sites in a notional volume containing both overlapping crystallites can be coincident in each lattice. Grain boundaries between two such misoriented lattices can therefore be highly ordered with narrow widths. The fraction of coincident sites is denoted by the Σ of the misorientation, defined such that a $\Sigma = n$ misorientation will have a fraction $1/n$ of coincident sites. There is considerable evidence that boundaries with low Σ values have properties differing (often favorably) from those of other boundaries [2, 3]. To include this information into the model, it will be necessary to define a discrete step function $S_k^{\mathrm{d-CSL}}$ which defines the number and type of each CSL. The Hamiltonian is then modified to include this in the same way as GNBs were included in equation (5), except no further binning is required in this case as this is already taken care of by the acceptance criterion that is imposed to define a CSL boundary [28]. Once this is incorporated it will be possible to explore, for example, the maximum fraction attainable in a microstructure of a given selection of CSL boundaries (this is possible analytically only for just $\Sigma = 3$ boundaries). The microstructures produced can then again be fed into a materials model to predict the benefit (or otherwise) of such configurations.

Two other refinements of the algorithm can also be addressed. First, the domain volumes are not explicitly included in the description of the texture. We swap orientations between domains but these domains are not of the same size so the texture is not strictly being conserved. When the microstructure is an equiaxed structure this will not be an important factor, but as we move to applying this model to less isotropic structures this effect will become important. Modifying the model to truly conserve texture will require us to abandon the description of texture as a collection of discrete orientations and replace it with an orientation distribution function (ODF).

Secondly, BMDs are defined in terms of the number fraction of boundaries rather than the area fraction. The distinction is irrelevant in systems where boundary area is independent of misorientation. However, when this is not the case BMDs constructed using number fraction may be misleading especially when linking BMDs to materials properties, such as corrosion resistance. This is an area where three-dimensional computer models with their ability to measure both area fraction and number fraction can be very useful. We intend to characterize, using this algorithm, the type of

microstructures in which boundary area becomes important in defining BMDs.

5. CONCLUSIONS

The algorithm is a computationally efficient way of incorporating texture and misorientation distribution functions into three-dimensional microstructural models. It bypasses the problem of boundary correlation, discussed in Section 1, by treating the system as a statistical ensemble and using a Monte Carlo method to evolve the state of the system toward the desired BMD. We have used the model to create a number of complex artificial BMDs using both conserved and non-conserved textures. The model has been applied successfully to create an experimentally obtained heterogeneous BMD in which two types of boundary are present. The inclusion into the model of boundary area, volume and CSL type is identified as the next step for the algorithm development.

Acknowledgements—This work was performed at Sandia National Laboratories, supported by the U.S. Department of Energy under contract number DE-AC04-94AL85000.

REFERENCES

1. Weiland, H., Adams, B. L. and Rollett, A. D. (ed.), *Proc. of the Third International Conference on Grain Growth*. TMS, Warrendale, PA, 1998.
2. Palumbo, G., Lehockey, E. M. and Lin, P., *J. Mater*., 1998, **50**(2), 40.
3. Schwartz, A. J. and King, W. E., *J. Mater*., 1998, **50**(2), 50.
4. Palumbo, G., King, P. J. and Lichtenberger, P. C., *Scripta metall. mater*., 1991, **25**, 1775.
5. Lin, P., Palumbo, G., Erb, U. and Aust, K. T., *Scripta metall. mater*., 1995, **33**, 1387.
6. Gertsman, V. Y., Zhilyaev, A. P., Pshenichnyuk and Valiev, R. Z., *Acta metall. mater*., 1992, **40**, 1433.
7. Garbacz, A. and Grabski, M. W., *Scripta metall. mater*., 1989, **23**, 1369.
8. Haraze, J. and Shimizu, R., *Acta metall*., 1990, **38**, 1395.
9. Becker, R. and Panchanadeeswaran, S., *Textures and Microstructures*, 1989, **10**, 167.
10. Frank, F. C., in *Eighth International Conference on Textures of Materials*, ed. J. S. Kallend and G. Gottstein. TMS, Warrendale, PA, 1987, pp. 3–16.
11. Krieger Lassen, N. C., Juul Jensen, D. and Conradsen, K., *Scanning Microscopy*, 1992, **6**, 115.
12. Adams, B. A., Wright, S. I. and Kunze, K., *Metall. Trans. A*, 1992, **24A**, 819.
13. Adams, B., *Mater. Sci. Engng*, 1993, **A166**, 59.
14. Pan, Y. and Adams, B. L., *Scripta metall. mater*., 1994, **30**, 1055.
15. Liu, Q., *Ultramicroscopy*, 1995, **60**, 1.
16. Hughes, D. A., Liu, Q., Chrzan, D. C. and Hansen, N., *Acta mater*., 1997, **45**, 105.
17. Hughes, D. A., Chrzan, D. C., Liu, Q. and Hansen, N., *Phys. Rev. Lett*., 1998, **81**, 4664.
18. Ling, S. and Anderson, M. P., *J. Mater*., 1992, **44**(9), 30.
19. Anderson, M. P., Grest, G. S. and Srolovitz, D. J., *Scripta metall*., 1985, **19**, 225.
20. Hansen, J., Pospiech, J. and Lucke, K., *Tables for Texture Analysis of Cubic Materials*. Springer-Verlag, Berlin, 1978.
21. Mackenzie, J. K., *Acta metall*., 1964, **12**, 223.
22. Kiewel, H., Bunge, H. J. and Fritsche, L., *Textures Microstruct*., 1996, **28**, 105.
23. Binder, K., *Monte Carlo Methods in Statistical Physics*. Springer-Verlag, New York, 1979.
24. Krieger Lassen, N. C., Juul Jensen, D. and Conradsen, K., *Acta crystallogr*., 1994, **A50**, 741.
25. Humphreys, F. J. and Hatherly, M., *Recrystallisation and Related Annealing Phenomena*. Pergamon Press, Oxford, 1995, p. 25.
26. Was, G., Thaveeprungsriporn, V. and Crawford, D. C., *J. Mater*., 1998, **50**(2), 44.
27. Sutton, A. P., *Int. metall. Rev*., 1984, **29**, 377.
28. Brandon, D. G., *Acta metall*., 1966, **14**, 1479.